Effect of Blowing Flow Control and Front Geometry Towards the Reduction of Aerodynamic Drag on Vehicle Models

Rustan Tarakka
Assistant Professor
Hasanuddin University
Department of Mechanical Engineering
Indonesia

Nasaruddin Salam
Professor
Hasanuddin University
Department of Mechanical
Indonesia

Jalaluddin
Associate Professor
Hasanuddin University
Department of Mechanical Engineering
Indonesia

Muhammad Ihsan
Lecturer
Sekolah Tinggi Teknik Baramuli
Department of Civil Engineering
Indonesia

This paper presents analyses of the effect of blowing flow control and variations on front geometry towards the reduction of aerodynamic drag on vehicle models. Blowing flow control is an alternative measure in modifying the onset of flow separation in the boundary layer on the surface of the vehicle. The modification is expected to reduce the dominating influence of the separation area on the total drag. Conducted in computational and experimental approaches, the research investigated the effect of frontal slant angle variations (θ) of 25°, 30° and 35° towards the reduction of aerodynamic drag on vehicle models on the application of blowing flow control with upstream and blowing speed of 16.7 m/s and 0.5 m/s, respectively. Load cells were used in the experimental method to validate the reduction of aerodynamic drag obtained from computational method. It is indicated that the effects of blowing flow control and variations on front geometry are significant in the increasing on pressure coefficients and the reduction of aerodynamic drag on vehicle models. The largest increase on pressure coefficients of 38.93% is indicated on the vehicle model with θ=35°, while the largest reduction of aerodynamic drag occurred on the same model with the values of 14.81 and 12.54 for computational and experimental methods, respectively.

Keywords: *active flow control, aerodynamic drag reduction, blowing, front geometry, vehicle model.*

1. INTRODUCTION

As one of the most preferred types of general vehicles, family car in the form of multi-purpose van (MPV) has both advantages and drawbacks. Of the drawbacks, one typical character is the demand of relatively larger capacity engine which means larger fuel consumption than its more compact counterparts. This type also generally has the basic shape of the bluff body to maximize the space volume of the passenger compartment. In terms of aerodynamics, this form results in larger aerodynamic drag due to the occurrence of enormous flow separation in rear parts of the vehicle body creating higher energy consumption of the vehicle. The aerodynamic drag contributes about half of mechanical energy expenditures of vehicles running at average highway speed of around 55 to 60 mph [1].

Ahmed vehicle model is an extremely simplified bluff-body model frequently used as a benchmark in vehicle aerodynamics research. A number of experimental research [2-6] and numerical studies [7-12] have been performed using the Ahmed model. One of the techniques under development to reduce aerodynamic drag on vehicles and to modify the generation of flow separation in the boundary layer on the surface of the vehicle which resulted in the generation of a backflow around the vehicle is the active flow control application. Active control strategies involve the addition of energy which aims to control, either in the form of prevention or inhibiting, the occurrence of flow separation which may lead to backflow on the surface of the vehicle without changing the shape of vehicles [13].

Some active control techniques have been developed and focusing on local intervention in wall turbulence dealing with steady blowing or suction [14-22]. Krentel et al. modeled a predictive closed-loop actuation approach for one steady blowing excitation configuration [16]. Harinaldi et al. [23] used a modified or reversed Ahmed body equipped with active flow control by blowing and found that the drag reductions achieved by computational and experimental methods were 13.92% and 11.11%. A review has also been elaborated for methods for the application of flow control on a square back car model [24]. This study aimed to analyze the effect of blowing active control incorporating the variations on front geometry towards the reduction aerodynamic drag on vehicle models. Improved reduction of aerodynamic drag can reduce flow separation which in turns will lead to energy efficiency. Comprehension of aerodynamic drag reductions and pressure coefficients are expected to improve the design method of future vehicles.

2. METHODOLOGY

The study investigates drag reduction occurring in a bluff body of van model adapted from Ahmed model, in

Received: November 2018, Accepted: March 2019
Correspondence to: Dr Rustan Tarakka
Department of Mechanical Engineering,
Jl. Poros Malino, Gowa, Indonesia
E-mail: rustan_tarakka@yahoo.com
doi: 10.5937/fmet1903552T

which flow streams in reversed direction from the original model or in other names, reversed Ahmed model [23, 25-28]. The van model was equipped with an active control by applying blowing techniques. Reversed Ahmed body model was chosen since it is a good representation of typical forms of popular family van produced by car manufacturer. The van model was investigated in both computational method, or CFD, and experimental method.

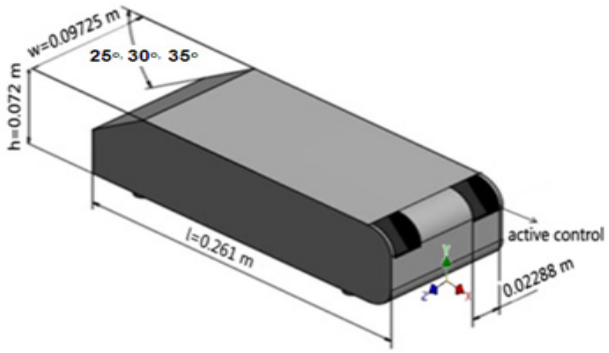

Figure 1. Reversed Ahmed body vehicle model

Figure 1 represents the basic vehicle model employed in the research with a 0.25 geometric ratio to the original Ahmed body model [2]. The vehicle model geometry was defined by its length (l=0.261m), width (w=0.09725 m) and its height (h=0.072 m). In this configuration, the front part of model was inclined with slant angles (θ) of 25°, 30° and 35°relative to the horizontal reference.

The value of viscous drag force and pressure drag force F_d is denoted in the equation (1).

$$F_d = \int \tau_w \sin\theta dS + \int p\cos\theta dS \tag{1}$$

while, drag coefficient C_d is expressed in the equation (2).

$$C_d = \int \frac{\tau_w}{\frac{1}{2}\rho V_\infty^2 S}\sin\theta dS + \frac{\int Cp\cos\theta dS}{S} \tag{2}$$

where $\tau_w = \mu(du/dy)_w$ is the wall shear stress which is assessed from the velocity gradient at the wall and $C_p = (p-p_\infty)/(\rho V_\infty^2/2)$ is pressure coefficient which is assessed from pressure distribution at the wall.

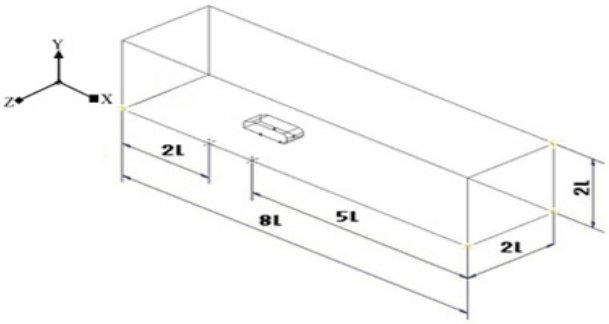

Figure 2. The 3D computational domain

The applied 3D computational domain is as shown in figure 2 denoting dimensions of length (L)=8l, width (W)=2l, and height (H)=2l, where l is the length of model in x-axis. This computation approach utilizes standard k-epsilon turbulence model as described on equation (3) for kinetic energy and equation (4) for dissipation rate.

$$\frac{\partial}{\partial t}(\rho k)+\frac{\partial}{\partial x_i}(\rho k u_i)=\frac{\partial}{\partial x_j}\left[\left(\mu+\frac{\mu_t}{\sigma_k}\right)\frac{\partial k}{\partial x_j}\right]+ \tag{3}$$
$$+P_b-\rho_\varepsilon+Y_M+S_k$$

$$\frac{\partial}{\partial t}(\rho\varepsilon)+\frac{\partial}{\partial x_i}(\rho\varepsilon u_i)=\left[\left(\mu+\frac{\mu_t}{\sigma_\varepsilon}\right)\frac{\partial\varepsilon}{\partial x_j}\right]+ \tag{4}$$
$$+c_{1\varepsilon}\frac{\varepsilon}{k}(P_k+C_{3\varepsilon}P_b)-C_{2\varepsilon}\rho\frac{\varepsilon^2}{k}+S_\varepsilon$$

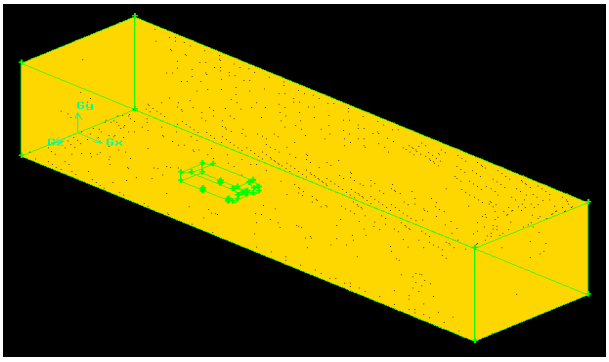

a. Vehicle model with θ=25°

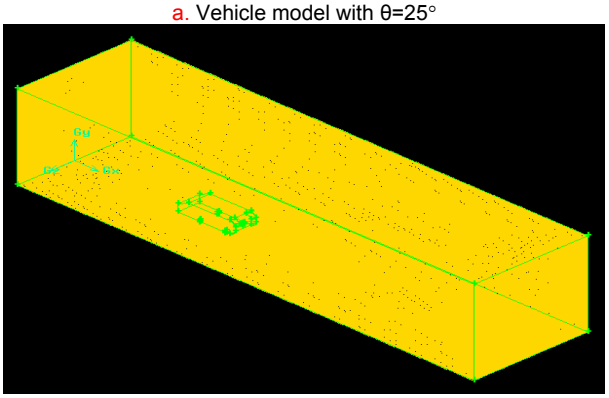

b. Vehicle model with θ=30°

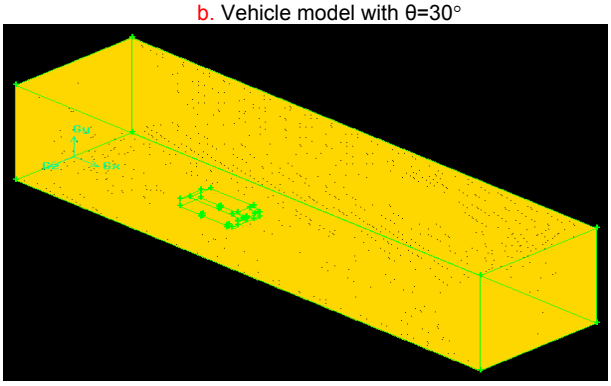

c. Vehicle model with θ=35°

Figure 3. Meshing on models with blowing control

Figure 3 shows the meshing on respective vehicle models with the application of blowing on the rear part of models. The type of meshing was tetra/hybrid element with hexcore type, where the number of mesh volume for the model with θ=25°was 2,321,940, while for models with θ=30° and θ=35° the number of mesh were 2,274,917 and 2,319,492 respectively. Inlet velocity of 16.7 m/s is assigned as the boundary condition. Average free stream at upstream region was

assumed to be in a steady state and uniform condition. The blowing speed was defined in0.5 m/s. Reynolds number corresponding to the length of the test model was at Re=2.98x10^5. The detailed computational conditions are given in table 1.

Table 1. Description of computational condition

Vehicle model	3D, steady state θ=25^o, θ=30^o andθ=35^o	
Fluid	Air	
Fluid properties	Density Viscosity	1.225 kg/m^3 0.000017894 kg/m-s
Boundary condition without an active flow control	Vehicle model Outlet Inlet Wall	Wall Pressure outlet Velocity inlet Wall
Boundary condition with blowing flow control	Vehicle model Outlet Inlet Wall Blowing1 Blowing2	Wall Pressure outlet Velocity inlet Wall Velocity inlet Velocity inlet
Upstream velocity	16.7 m/s	
Blowing velocity	0.5 m/s	

The tests were conducted in a controlled subsonic wind tunnel supplied with free stream air flow, testing acrylic van model with a 0.25 scale to the original Ahmed body model [2]. The wind tunnel has been calibrated complying manufacturer specification and considering recommendation by several works [29-31]. The van models are classified as models without flow control and models with blowing flow control. The blowing apparatus was configured at the internal part of the body of the model where the flow separation was predicted by computational method to induce a significant drag. The blowing apparatus was operated by using a mini compressor with blowing velocity at 0.5 m/s.

The investigated parameter was the aerodynamic drag force measured by using a load cell. Prior to the main experiments, the load cell was calibrated by using a digital balance. A preliminary measurement was performed to determine the statistical uncertainty of force measurements which was predicted to range at about ± 2%. The setup for the aerodynamic drag force measurement is as shown in figure 4.

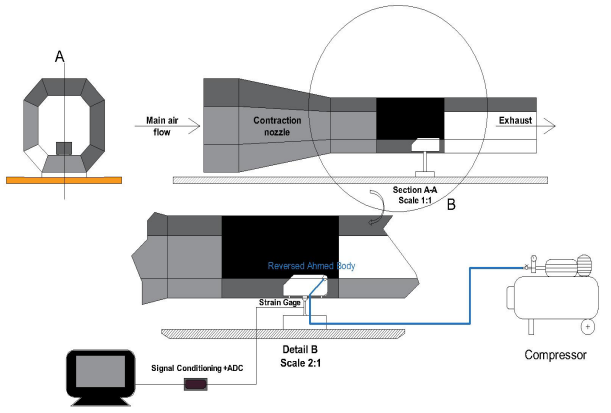

Figure 4. Experimental setup for the aerodynamic drag force measurement

Dimensionless drag coefficient relative to drag force working on the bluff body is defined in the equation (5):

$$C_d = \frac{F_d}{\frac{1}{2}\rho V_\infty^2 S} \tag{5}$$

where, ρ is air density, V_∞ is free stream velocity, S is cross sectional area and F_d is the total drag force working on vehicle models as measured by the load cell.

3. RESULTS AND DISCUSSION

Main results of the research are pressure coefficients and aerodynamic drags which evaluated in terms of reduction in the application of blowing active control. Figure 5 presents contour pathlines coloured by static pressure for models without active flow control for respective front slant angles.

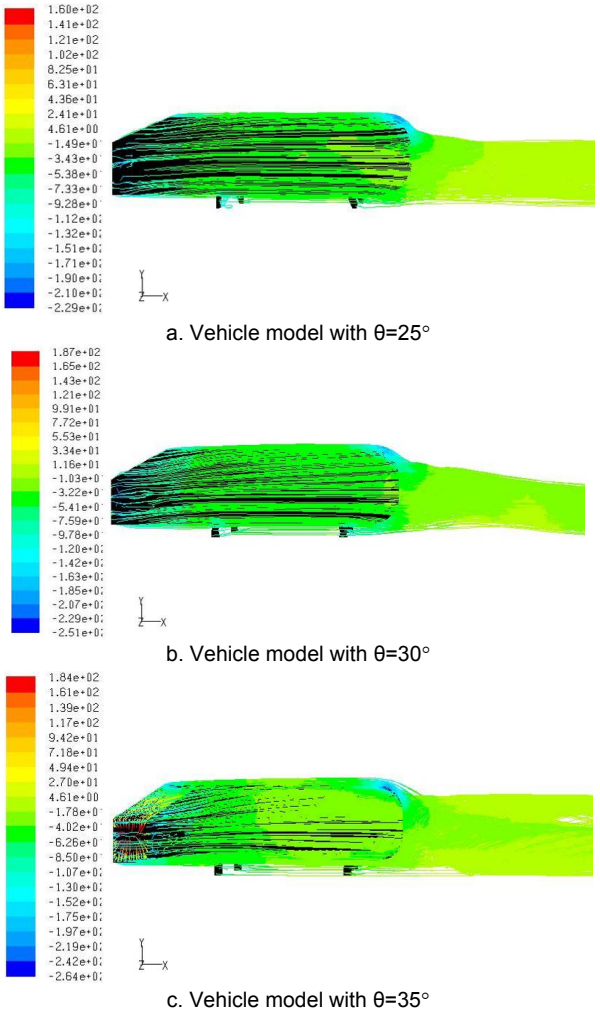

Figure 5. Pathlines colored by static pressure without active flow control

The relationships of flow characteristics and vehicle's geometric parameters are presented in consecutive figures and tables. The first to be discussed is the expression of the distribution of pressure coefficient C_p in the relation to the so-called y/h ratio which is the ratio of the height of the grid to the height of vehicle model. The second will be the patterns of pressure coefficient distribution on the rear part of vehicle models in

regards with z/w parameter, the ratio of width of grid to the width of vehicle models. The first one is shown in figure 6 for vehicle models with slant angle variations (θ) of 25°, 30° and 35° and given upstream velocity of 16.7 m/s.

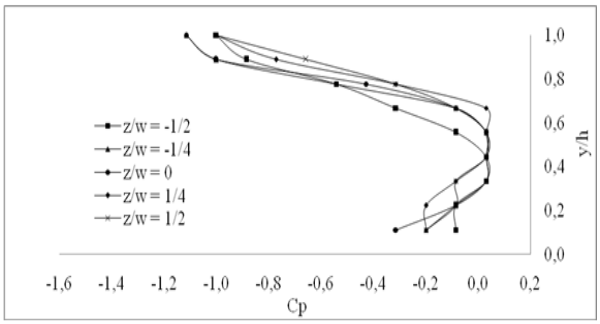

Vehicle model with θ=25°

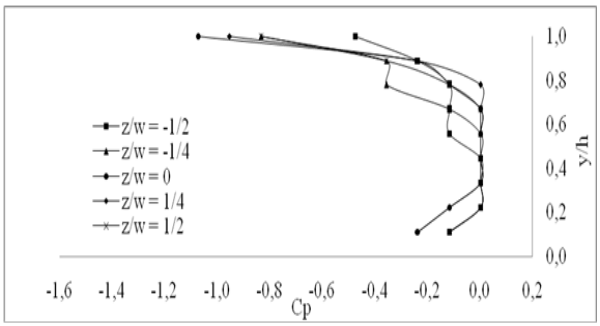

Vehicle model with θ=30°

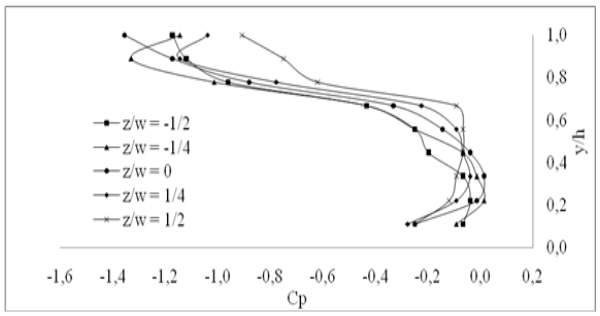

Vehicle model with θ=35°

Figure 6. The distribution of pressure coefficients without an active flow control

The minimum values of pressure coefficients on respective test model are presented in table 2 where, as shown in the table 2, the minimum value of pressure coefficients occurs at y/h=1, specifically on the edge of upper side of rear part of respective vehicle models. The highest pressure coefficient is recorded on the vehicle model with a 30° front slant angle as compared to the coefficients on models with 25°and 35°frontal slant angles. It is expected that a flow separation is likely to occur on the rear part of vehicle models, where the separation could induce back flow and therefore can reduce the pressure coefficient. This evidence is in agreement with the opinion of Anderson et al. [32].

Table 2, The minimum value of pressure coefficients without an active flow control

Vehicle model	Pressure coefficient, C_p	y/h	z/w
$\theta=25^0$	-1.1148	1	-1/4 and 0
$\theta=30^0$	-1.0716	1	0
$\theta=35^0$	-1,3556	1	0

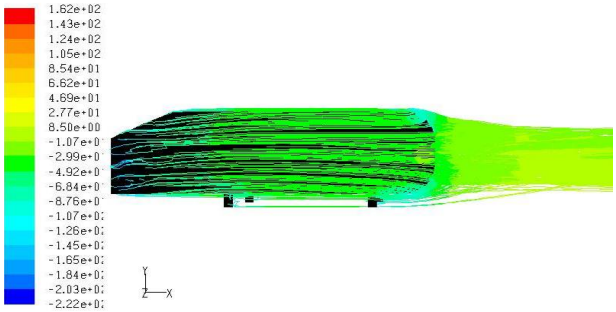

Vehicle model with θ = 25°

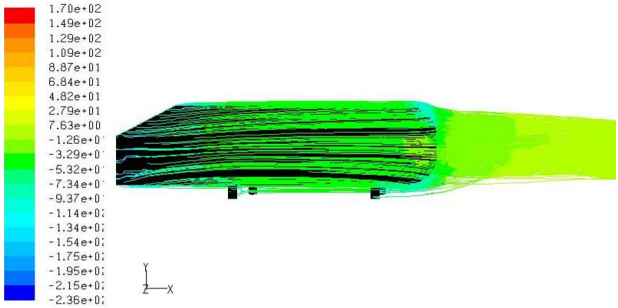

Vehicle model with θ = 30°

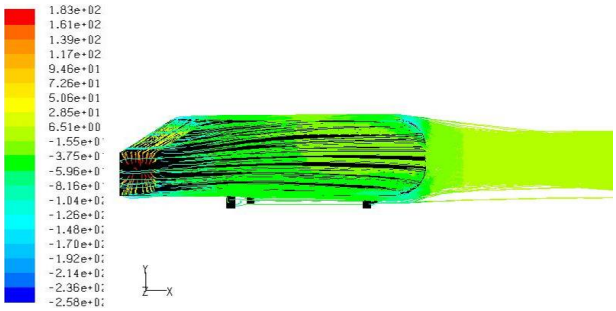

Vehicle model with θ = 35°

Figure 7. Pathlines colored by static pressure with blowing flow control

The presence of active control in the form of blowing was then evaluated based on the same parameter. Figure 7 presents contour pathlines colored by static pressure for models with the application of blowing active flow control for respective front slant angles. Figure 8 presents the distributions of pressure coefficients for given 16.7 m/s upstream velocity U_o as well as 0.5 m/s blowing velocity U_{bl}; all were applied on vehicle models with frontal slant angles of 25°, 30° and 35° respectively.

The figures show that with the application of blowing flow control, the pressure coefficient tends to increase. From around y/h=0.6 to y/h=1, pressure coefficients start to change in a positive direction. This finding shows that on the upper side of the rear part of respective model, pressure coefficient increases. By the application of blowing flow control, the lower pressure stream, and considering the shape factor and friction of air with model's wall can be reduced therefore the flow separation the rear part of the test model can be reduced as well. Table 3 summarizes the minimum values of the pressure coefficient distribution on a 0.5 m/s given blowing velocity U_{bl} and a 16.7 m/s upstream velocity U_o. The table also shows that the smallest pressure coefficient distribution was on the model with a 30° front slant angle when compared to the test model with 25° and 35° slant angles.

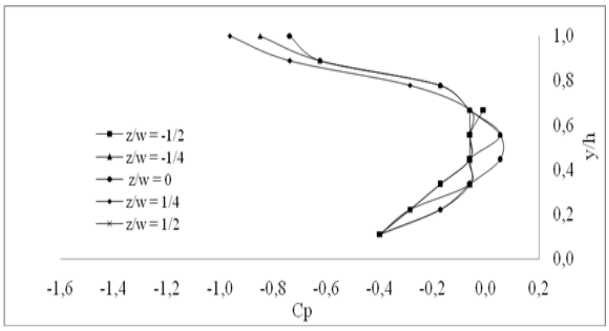

Vehicle model with θ = 25°

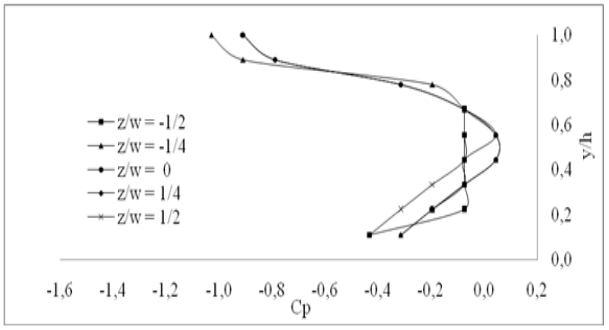

Vehicle model with θ = 30°

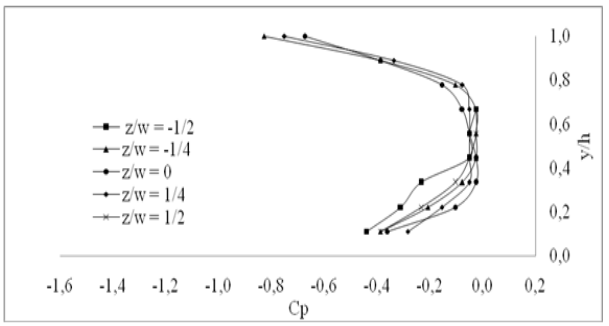

Vehicle model with θ = 35°

Figure 8. Pressure coefficient distribution with blowing flow control

Table 3. Minimum values of pressure coefficient with blowing flow control

Vehicle model	Pressure coefficient, C_p	y/h	z/w
$\theta=25^0$	-0.9622	1	1/4
$\theta=30^0$	-1.0285	1	-1/4
$\theta=35^0$	-0.8279	1	-1/4

The effect of additional active control by blowing with U_{bl}=0.5 m/s blowing speed in the reduction of the flow separation at the rear of each vehicle model is shown in table 4. The reduced flow separation gives an effect in the increase of the pressure coefficients on all vehicle models [33].

Table 4. Increasing pressure coefficient with blowing flow control

Vehicle model	Pressure coefficient, C_p		Increasing C_p, (%)
	Without active flow control	With blowing	
$\theta=25^0$	-1.1148	-0.9622	13.69
$\theta=30^0$	-1.0716	-1.0285	4.02
$\theta=35^0$	-1,3556	-0.8279	38.93

The largest value of increasing of pressure coefficient with the addition of blowing active control is on the model with 35° front slant angle gaining a number of percentages of 38.93%.

3.1 The computational method

Table 5 presented the aerodynamic drag coefficients for computational approach on the vehicle models with frontal slant angle of θ=25°, θ=30° and θ=35° both for normal treatment (without flow control) and with the addition blowing flow control with blowing speed U_{bl} of 0.5 m/s and upstream velocity U_o of 16.7 m/s.

Table 5. Aerodynamic drag coefficient and aerodynamic drag reduction by computational method

Vehicle model	Aerodynamic drag coefficient, C_d		Aerodynamic drag reduction, %
	without active flow control	with blowing	
$\theta=25^0$	1.7752	1.5639	11.90
$\theta=30^0$	1.6709	1.5699	6,04
$\theta=35^0$	1.7556	1.4953	14.81

Table 5 gives information that, in vehicle model without active control, the smallest aerodynamic drag coefficient is obtained in model with a 30° slant angle with the value of 1.6709 while on the models with 25° and 35° front slant angles, aerodynamic drag coefficients were 1.7752 and 1.7556 respectively. It is shown that the aerodynamic drag coefficients on each model were decreasing as the effect of the additional blowing active control while the smallest drag coefficient occurred in the model with θ=35°where the value of 1.4953. For models with θ=25° and θ=30°, the aerodynamic drag coefficients were 1.5639and 1.5699 respectively.

From the table 5 also, the largest reduction of aerodynamic drag as the effect of blowing flow control occurs on vehicle model with θ of 35° on a given 0.5 m/s blowing velocity U_{bl} and 16.7 m/s upstream velocity U_o with the reduction percentage was 14.81% . For the vehicle models with slant angles of 25°and 30°, the reduction were 11.90% and 6.04% respectively, as shown in table 5. The aerodynamic drag value on vehicle model with front slant angle 35° is capable to increase pressure coefficient on rear part of vehicle model for up to 38.93% as the effect of blowing flow control. The increasing of pressure coefficient on rear parts of vehicle models can decrease the aerodynamic drag. Results obtained from the research have confirmed the results of other researchers [16, 18, 23, 26, 27] where the application of active control by blowing can reduce aerodynamic drag on vehicle models.

3.2 The experimental method

Table 6 presents the aerodynamic drag coefficients obtained from experimental method on three vehicle models, which have similar geometric parameters to the model used for computational method.

Table 6 gives the information that for models without flow control, the smallest aerodynamic drag coefficients occurs in the 30° front slant angle vehicle model with 1.5173 value as for models with θ=25°and θ=35°,

the aerodynamic drag coefficients were 1.6237 and 1.5655 respectively. Additional blowing flow control for all models gives reduction of aerodynamic drag coefficients while the smallest aerodynamic drag coefficients occurred in the model with a 35°front slant angle with the value of 1.3747% and 1.4480% as well as 1.4313% for vehicle models with θ=25° and θ=30°.

Table 6. Aerodynamic drag coefficient and aerodynamic drag reduction by experimental method

Vehicle model	Aerodynamic drag coefficient, C_d		Aerodynamic drag reduction, %
	without active flow control	with blowing	
$\theta=25^0$	1.6237	1.4480	10.82
$\theta=30^0$	1.5173	1.4313	5.67
$\theta=35^0$	1.5655	1.3747	12.54

From the table 6 also, it is obvious that the smallest reduction of aerodynamic drag by active control with blowing speed U_{bl} of 0.5 m/s and upstream velocity U_o of 16.7 m/s occurred on the model with θ=35° giving the reduction of 12.54% while on models with θ=25° dan θ=30° the reductions were 10.82% and 5.67% respectively.

The comparison of aerodynamic drag coefficients for vehicle models with θ=25°, θ=30°and θ=35° front slant angles obtained from both computational method as well as experimental method are shown on tables 7, 8 and 9 respectively.

Table 7 contains the comparison of aerodynamic drag coefficient for vehicle model with slant angle θ=25° from computational and experimental methods. It is shown that the aerodynamic drags coefficients from the two methods on models without flow control differ in about 8.53%, as for models with a 0.5 m/s blowing flow control, the two methods result a 7.41% difference in the value of aerodynamic drag coefficient. The table 7 also informs that there is a 1.08% slight difference in the reduction of aerodynamic drag coefficient for the two methods.

Table 7. Aerodynamic drag coefficient (C_d) for vehicle model with $\theta=25^0$

Description	Aerodynamic drag coefficient, (C_d)		Aerodynamic drag coefficient (C_d) reduction (%)
	without active flow control	with blowing	
Computational	1.7752	1.5639	11.90
Experimental	1.6237	1.4480	10.82
Difference	8.53%	7.41%	1.08

Table 8 shows the comparison of aerodynamic drag coefficients from both computational and experimental approaches for vehicle model with slant angle of θ=30°.The coefficients of aerodynamic drag of the two methods for models without flow control differ on 9.19% differences. For vehicle models with blowing flow control at blowing speed of 0.5 m/s, the two methods give 8.83% difference in aerodynamic drag coefficient values. The table 8 also shows that the reduction of aerodynamic drag coefficients between computational and experimental methods differ on only 0.37%.

Table 8. Aerodynamic drag coefficient (C_d) for vehicle model with $\theta=30^0$

Description	Aerodynamic drag coefficient, (C_d)		Aerodynamic drag coefficient (C_d) reduction (%)
	without active flow control	with blowing	
Computational	1.6709	1.5699	6.04
Experimental	1.5173	1.4313	5.67
Difference	9.19%	8.83%	0.37

Table 9. Aerodynamic drag coefficient (Cd) for vehicle model with θ=350

Description	Aerodynamic drag coefficient, (C_d)		Aerodynamic drag coefficient (C_d) reduction (%)
	without active flow control	with blowing	
Computational	1.7556	1.4953	14.81
Experiment	1.5655	1.3706	12.54
Difference	10.82%	8.34%	2.27

Aerodynamic drag coefficients obtained from computational and experimental methods for θ=35° model are listed in table 9. For models without flow control, the aerodynamic drag coefficients of the two methods have 10.82% differences. On vehicle models with active blowing flow control at blowing speed of 0.5 m/s, the two methods give 8.34% difference in aerodynamic drag coefficient values. The table 9 also shows that the reductions of aerodynamic drag coefficients of the two methods differ about 2.27%.

4. CONCLUSION

Based on the results of pressure coefficients and drag reduction on reversed Ahmed vehicle models with front slant angles (θ) of 25°, 30° and 35° as well as the application of blowing flow control, some conclusion can be drawn. It is obvious that the active flow control by blowing and variations on front geometry provide significant impact to the increasing of pressure coefficients and reduction of aerodynamic drag. The most significant increase on pressure coefficients occurs on vehicle model with the 35° front slant angle, gaining 38.93% value, where pressure coefficients with and without blowing flow control reach -0.8279 and -1.3556, respectively. In terms of aerodynamic drag reduction, vehicle model with the 35° front slant angle also gains the value of 14.81 and 12.54 for computational and experimental methods, while the reductions of aerodynamic drag coefficients of the two approaches have 2.27% difference.

ACKNOWLEDGEMENTS

The research was funded by the Ministry of Research, Technology and Higher Education, The Republic of

Indonesia, through University Excellence Scheme F.Y 2018, with Research Contract No. : 1579/UN4.21/PL. 00.00/2018, dated March 21th 2018.

REFERENCES

[1] Agarwal, R.K."Sustainable ground transportation – review of technologies, challenges and opportunities", International Journal of Energy and Environment, Vol. 4, No.6, pp.1061-10782013, 2013.

[2] Ahmed, S., Ramm, G., Faltin, G."Some Salient Features Of The Time-Averaged Ground Vehicle Wake", SAE Technical Paper 840300, 1984.

[3] Sims-Williams, D., Dominy, R. "Experimental Investigation into Unsteadiness and Instability in Passenger Car Aerodynamics", SAE Technical Paper 980391, 1998.

[4] Bayraktar, I., Landman, D., Baysal, O. "Experimental and Computational Investigation of Ahmed Body for Ground Vehicle Aerodynamics", SAE Technical Paper 2001-01-2742, 2001.

[5] Joseph, P., Amandolese, X., Edouard, C. Aider, J. "Flow control using MEMS pulsed micro-jets on the Ahmed body", Experiment in Fluids, Vol. 54, No. 1, 1442, 2013.

[6] Lienhart, H., Becker, S. "Flow and Turbulence Structure in the Wake of a Simplified Car Model", SAE Technical Paper 2003-01-0656, 2003,

[7] Han, T. "Computational analysis of three-dimensional turbulent flow around a bluff body in ground proximity", AIAA Journal, Vol. 27, No.9, 1989, pp. 1213-1219.

[8] Basara, B., Przulj, V., Tibaut, P. "On the Calculation of External Aerodynamics: Industrial Benchmarks", SAE Technical Paper 2001-01-0701, 2001.

[9] Basara, B. "Numerical simulation of turbulent wakes around a vehicle", in: *ASME Fluid Engineering Division Summer Meeting FEDSM99-7324*. San Francisco, USA, 1999.

[10] Basara, B., Alajbegovic, A. "Steady state calculations of turbulent flow around Morel body". in: *7th International Symposium of Flow Modelling and Turbulence Measurements*, Taiwan, 1998, pp. 1–8

[11] Gilliéron, P.,Chometon, F. "Modeling of stationary three-dimensional separated air flows around an Ahmed reference model", in : *ESAIM, Proceeding of Third International Workshop on Vortex Flows and Related Numerical Methods*, 7, 1999, pp. 173–182.

[12] Kapadia, S., Roy, S., Vallero, M., Wurtzler, K., Forsythe J. "Detached-Eddy Simulation over a Reference Ahmed Car Model", in: Friedrich, R., Geurts, B.J., Métais, O. (eds*) Direct and Large-Eddy Simulation V*. ERCOFTAC Series, 9. Springer, Dordrecht, 2004, pp 481-488.

[13] Conan, B., Anthoine, J., Planquart, P. "Experimental aerodynamic study of a car-type bluff body", Experiments in Fluids, Vol. 50, No. 5, pp.1273-1284, 2010.

[14] Krogstad, P.A., Kourakine, A. "Some effects of localized injection on the turbulence structure in a boundary layer", Physics of Fluids, Vol. 12, No.11, pp. 2990-2999, 2000.

[15] Park, J., Choi, H. "Effects of uniform blowing through blowing or suction from a spanwise slot on a turbulent boundary layer flow", Physics of Fluids, Vol. 11, No. 10, pp. 3095–3105, 1999.

[16] Krentel D., Muminovic R., Brunn A., Nitsche W., King R. "Application of Active Flow Control on Generic 3D Car Models". in: King R. (eds) *Active Flow Control II. Notes on Numerical Fluid Mechanics and Multidisciplinary Design*, 108. Springer, Berlin-Heidelberg, Germany, 2010, pp. 223-239.

[17] Heinemann, T., Springer, M., Lienhart, H. "Active flow control on a 1:4 car model", Experiments in Fluids, Vol. 55, No. 5, 1738, 2014.

[18] Mestiri, R., Ahmed-Bensoltane, A., Keirsbulck, L., Aloui, F.,Labraga, L. "Active Flow Control at the Rear End of a Generic Car Model Using Steady Blowing", Journal of Applied Fluid Mechanics, Vol. 7, No. 4, pp. 565-571, 2014.

[19] Tounsi, N., Mestiri, R., Keirsbulck, L., Oualli, H., Hanchi, S., Aloui, F."Experimental Study of Flow Control on Bluff Body using Piezoelectric Actuators" , Journal of Applied Fluid Mechanics , Vol. 9, No. 2, pp. 827-838, 2016.

[20] Tian, J., Zhang, Y., Zhu, H., Xiao, H."Aerodynamic drag reduction and flow control of Ahmed body with flaps", Advances in Mechanical Engineering, Vol. 9, No.7, pp. 1–17, 2017.

[21] Shadmani, S., Mousavi-Nainiyan, S.M., Ghasemiasl, R.,Mirzaei, M., Pouryoussefi, S.G. "Experimental Study of Flow Control Over an Ahmed Body Using Plasma Actuator", Mechanics and Mechanical Engineering, Vol. 22, No. 1, pp. 239–251, 2018.

[22] Prakash, B., Bergada, J.M., Mellibovsky, F. "Three Dimensional Analysis of Ahmed Body Aerodynamic Performance Enhancement using Steady Suction and Blowing Flow Control Techniques", in : *Tenth International Conference on Computational Fluid Dynamics (ICCFD10)*, 2018. Barcelona, Spain.

[23] Harinaldi, Budiarso, Tarakka, R., Simanungkalit, S.P. "Effect of Active Control by Blowing to Aerodynamic Drag of Bluff Body Van Model", International Journal of Fluid Mechanics Research, Vol. 40, No.4, pp. 312-323, 2013.

[24] Julian, J., Karim, R.F., Budiarso, Harinaldi, "Review: Flow Control on a Squareback Model" International Review of Aerospace Engineering (IREASE), Vol. 10, No. 4, pp. 230-239, 2017.

[25] Harinaldi, Budiarso, Warjito, Kosasih, E.A., Tarakka, R., Simanungkalit, S.P. "Active technique by suction to control the flowstructure over a van model", Journal of Engineering and Applied Science, Vol. 7, No. 2, pp.215-222, 2012.

[26] Harinaldi, Budiarso, Tarakka, R., Simanungkalit, S.P. "Computational Analysis of Active Flow Control to Reduce Aerodynamics Drag on a Van Model", International Journal of Mechanical & Mechatronics Engineering IJMME-IJENS, Vol. 11, No. 3, pp. 24-30, 2011

[27] Tarakka, R., Jalaluddin, Mire, B., Umar, M.N. "Effect of Turbulence Model In Computational Analysis of Active Flow Control on Aerodynamic Drag of Bluff Body Van Model", International Journal of Applied Engineering Research, Vol. 10, No. 1, pp. 207-219, 2015.

[28] Tarakka, R., Salam, N., Jalaluddin, Ihsan, M. "Active Flow Control by Suction on Vehicle Models with Variations on Front Geometry", International Review of Mechanical Engineering, Vol. 12, No. 2, 2018, pp. 128-134.

[29] Plint and Partners, Manual of Educational Wind Tunnel, England, 1982.

[30] Ocokoljić, G., Damljanović, D., Vuković, Đ., Rašuo, B. "Contemporary Frame of Measurement and Assessment of Wind-Tunnel Flow Quality in a Low-Speed Facility", FME Transactions, Vol. 46, No. 4, pp. 429-442, 2018.

[31] Ocokoljić, G., Damljanović, D., Rašuo, B., Isaković, J. "Testing of a Standard Model in the VTI's Large subsonic Wind-tunnel Facility to Establish Users' Confidence", FME Transactions, Vol. 42, No. 3, pp. 212-218, 2014.

[32] Anderson, J.D. "Fundamental of Aerodynamics" 3rd ed., McGraw-Hill, Singapore, 2001.

[33] Sphon, A., Gilliéron, P. "Flow separations generated by simplified geometry of an automotive vehicle", in: *IUTAM Symposium: Unsteady separated flows*, 2002, Toulouse, France.

NOMENCLATURE

Cd	drag coefficient
Cp	pressure coefficient
Fd	pressure drag force [N]
h	height of test model [m]
l	length of test model [m]
ρ	density [kg/m^3]
θ	front slant angle [^{o}]
Re	Reynolds number
S	cross section area [m^2]
τ_w	wall shear stress [N/m^2]
U_{bl}	blowing velocity [m/s]
U_o	upstream velocity [m/s]
μ	viscosity [N.s/m^2]
w	width of test model [m]

УТИЦАЈ РЕГУЛАЦИЈЕ ПРОТОКА ДУВАЊА И ПРЕДЊЕ ГЕОМЕТРИЈЕ НА СМАЊЕЊЕ АЕРОДИНАМИЧКОГ ОТПОРА КОД МОДЕЛА ВОЗИЛА

Р.Тарака, Н.Салам, Џалалудин, М.Ихсан

Анализира се утицај регулације протока дувања и варијације предње геометрије у циљу редукције аеродинамичког отпора код модела возила. Регулација протока дувања је алтернативна мера за модификацију почетка раздвајања протока у граничном слоју на површини возила. Очекује се да се модификацијом смањи доминантан утицај области раздвајања на укупан отпор. Истраживање извршено нумеричким и експерименталним методама се бави испитивањем утицаја варијација предњег нагибног угла од 25^0, 30^0 и 35^0 на редукцију аеродинамичког отпора код модела возила при регулацији протока дувања узлазно и брзине протока од 16,7 м/с односно 0,5 м/с. Мерне ћелије су коришћене код експеримента за евалуацију аеродинамичког отпора израчунатог нумеричком методом. Утврђено је да регулација протока дувања и варијације предње геометрије имају значајан утицај на повећање коефицијената притиска и смањење аеродинамичког отпора код модела возила. Највеће повећање коефицијената притиска од 38,93% је било код модела са нагибним углом од 35^0, док је највеће смањење аеродинамичког отпора било на истом моделу: од 14,81 – 12,54 применом нумеричке односно експерименталне методе.